Journal of Hydroscience and Hydraulic Engineering
Vol.12, No.2, November, 1994, 17-30

UNSTEADY NUMERICAL MODEL OF TWO-DIMENSIONAL STARTING PLUMES TRAVELLING DOWNSLOPE

BY

Juichiro Akiyama, Masaru Ura, and Sanit Wongsa

Department of Civil Engineering, School of Engineering
Kyushu Institute of Technology, Kitakyushu 804, Japan

SYNOPSIS

Layer-averaged equations describing the flow characteristics of a two-dimensional inclined starting plume, which consists of two parts,i.e. a front part and a body part, are derived. A hybrid numerical model is formulated on the basis of the characteristic method for the body part and the Runge-Kutta-Gill method for the front part, incorporating such empirical relationships as an entrainment function for the body part E_e as well as for the body part E_d and the height-to-length ratio(θ) of the front part. For the range of bottom slope angles θ =5~90° the model is calibrated with such empirical relationships as the dimensionless front propagation speed U_{fe}^*, the spatial growth rate for the body part dh/dx and for the front part dh_f/dx. The calculated results are then compared with an additional set of laboratory experimental data for the bottom slope angles θ =5.71° and 8.13° .

INTRODUCTION

In many problems of environmental interest, there are numerous practical situations in which a denser fluid is released into a less dense environment. This dense fluid spreads under the action of buoyancy force and forms a "gravity current." Typical examples of such phenomena are sea-breeze fronts, accidental release of dense industrial gases, powder-snow avalanches and turbidity currents. The difference in density that provides the driving force may be due to dissolved substances or temperature differences, or due to suspeded solid. A gravity current generated by dissolved substances or temperature differences is customarily called a "non-suspension type," whereas a gravity current resulting from suspended matter is called a "suspension type."

A gravity current travelling downslope can be in the form of either a "starting plume" or a "thermal," depending on whether the source is continuous or instantaneous. The starting plume consists of a head with complex three-dimensional structure at the leading edge, followed by a thinner flow. This leading edge is commonly called as a "front part," and the upstream of it is referred to as a "body part." There is a zone of low density due to mixed fluid left behind the current head. This part of the flow is referred to as a "mixed layer." On the other hand, the thermal consists only of a head structure, without a distinct body part. Among various forms of gravity currents the present study is concerned with prediction of the motion of a non-suspension two-dimensional starting plume flowing downslope. A non-suspension inclined starting plume is illustrated schematically in Fig.1 along with the coordinate system and the notation to be used.

A great deal of study has been devoted to predict the motion of inclined starting plumes (for instance, Britter & Linden(5), Fukuoka *et al.*(7), Fukushima(8), and Hirano & Hadano(9)). For practical applications, it is required to at least predict the front propagation speed U_{fe} or

alternatively the mass-centre velocity U_f, the height h_f of the front, and the density ρ_f or alternatively the buoyancy force of the front B_f. Fukuoka *et al.*(7) developed a model, consisting of the conservation of volume and unsteady momentum equation. The mass-centre velocity U_f and the maximum front height h_f were computed, treating the drag coefficient as a free parameter. Hirano & Hadano(9) proposed an analytical model based on gradually varied flow equation. Britter & Linden(5) proposed a simple analytical model to predict the front propagation speed relating the body part to the front part through the Bernoulli equation. Since Britter & Linden's model can predict only one of the flow characteristics,i.e. the front propagation speed, it can not be considered as a useful model, although findings reported therein are very significant. Fukushima(8) proposed a model for suspension inclined starting plumes by integrating two-phase(solid-fluid) flow equation. The model performance for non-suspension inclined starting plumes was examined, treating the drag coefficient as a free parameter. Research on inclined plumes conducted in Japan is concisely reviewed by Akiyama(3).

Each of the aforementioned model was validated by comparing calculated results with experimental data. Fukuoka *et al.*(7) compared the flow height h as well as the mass-centre velocity U_f in case of bottom slope angle θ =5.71° , Hirano & Hadano's model(9) was validated by comparing U_{fe} in case of θ=11.7° , Britter & Linden(5) compared the dimensionless front propagation speed U_{fe}^* for the range of bottom slope angles θ=5~90° , and Fukushima(8) compared h as well as U_{fe} in the case of θ =10° ,15° , and 30° . The drag coefficient was commonly treated as a free parameter and in some models more parameters were involved to obtain good agreement between calculated and experimental results. All of the aforementioned models, except the one proposed by Britter & Linden, were verified under restricted bottom slope angles. Thus, applicability of a model to other situations remains uncertain. Furthermore, validation of all of the models was achieved by examining only the velocity or both velocity and height of the front part; predictability of the density(buoyancy) remains totally uncertain.

A model is desired that predicts the height, density, and velocity of the flow by knowing inflow and bottom slope conditions under wide range of inflow and bottom slope conditions. From such a point of view, Akiyama *et al.*(1) proposed a model capable of simultaneously simulating height, density, and velocity for the front part as well as the body part under unsteady inflow conditions. When inclined starting plumes are set up by releasing a constant buoyancy flux, this model is very much simplified into the one by Akiyama & Ura(2). However, the model contains five model constants;the drag coefficient C_d, the entrainment function E_d, the velocity and buoyancy correction factor(k_U,k_B) for the front part and the friction coefficient f_b for the body part. These model constants were determined for the range of bottom slope angles θ =5~60° through model calibration. Such existing empirical results reported by Britter & Linden as spatial growth rate for the body part dh/dx and for the front part dh_f/dx as well as the dimensionless front propagation speed U_{fe}^* were used. In addition, two additional conditions were imposed to determine all of model constants; dh_f/dx=constant and dU_{fe}^*/dx=0 at large x.

This paper continues further investigation of Akiyama *et al.*'s model(1). With a view to reducing the number of the model constants and to improving model predictability, the following improvements are made in the present hybrid model. The former objective is attained by incorporating the entrainment function E_d for the front part into the present model and by setting k_B=0 on the basis of experimental evidence. The latter objective is attained by using the empirical results obtained by Akiyama *et al.*(4); incorporation of such empirical results as the entrainment function E_e for the body part and the length-to-height ratio $f(\theta)$ for the front part, and calibration of the present model with the spatial growth rate for the body part as well as for the front part(dh/dx,dh_f/dx) and the dimensionless front propagation speed U_{fe}^* for the range of bottom slope angle θ =5~90° . All of the aforementioned flow characteristics used for the present model were quantified based on a large volume of experimental

data(see Akiyama *et al.*(4) for detail), so that the reliability of the empirical results are substantially higher than those used in Akiyama *et al.*'s model(1).

MODEL FORMULATION

The motion of a two-dimensional inclined starting plume is represented by the model illustrated in Fig.1, where the coordinate system and the notation to be used are also presented. Denser fluid of density $\rho_a+\Delta\rho_f$ in the front part, together with density $\rho_a+\Delta\rho$ in the body part, flows down a slope of angle θ under an infinitely deep quiescent lighter fluid of density ρ_a. The mixed layer with density $\rho_a+\Delta\rho_m$ is left behind the front.

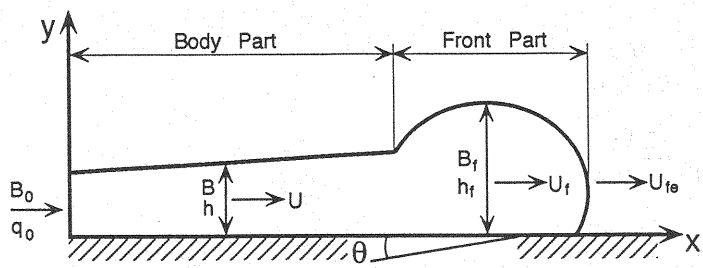

Fig.1 Definition Sketch of an Inclined Starting Plume.

For modelling the body part, the two-layer stratified analysis is employed. Under the assumption of hydrostatic pressure distribution along with boundary and Boussinesq's approximations, the layer-integrated governing equations of the body part are derived as follows;

$$\frac{\partial h}{\partial t}+\frac{\partial}{\partial x}(f_1Uh)=E_eU \tag{1}$$

$$\frac{\partial}{\partial t}(f_2Bh)+\frac{\partial}{\partial x}(f_3BUh)=0 \tag{2}$$

$$\frac{\partial}{\partial t}(f_1Uh)+\frac{\partial}{\partial x}(f_4hU^2)=f_2Bh\sin\theta-\frac{1}{2}\frac{\partial}{\partial x}(f_5Bh^2\cos\theta)-f_bU^2 \tag{3}$$

In the preceding equations, profile constants f_1~f_5 are introduced to account for the non-uniformity of velocity and buoyancy force distributions and are defined as follows;

$$f_1=\frac{1}{Uh}\int_0^\infty udy;\ f_2=\frac{1}{Bh}\int_0^\infty bdy;\ f_3=\frac{1}{BUh}\int_0^\infty budy;\ f_4=\frac{1}{hU^2}\int_0^\infty u^2dy;\ f_5=\frac{1}{Bh^2}\int_0^\infty 2bydy \tag{4}$$

In principle, the downstream development of the velocity U(x,t), thickness h(x,t), and buoyancy force B(x,t) of the body flow can be calculated by solving simultaneously Eqs. 1~3 togeter with supplemental relationships regarding the entrainment function E_e and the friction coefficient f_b under specified upstream conditions(U(0,t),B(0,t),h(0,t)).

There are a number of numerical methods for solving the preceding equations. Here, the

method of characteristics with specified-space-intervals is employed to solve Eqs.1 and 3, and the explicit finite difference to solve Eq.2. The original partial differential equations(Eqs.1 and 3) are transformed into a pair of characteristic equations on x-t plane and a pair of total differential equations, respectively.

$$\frac{dx}{dt} = \frac{f_1 h + \lambda(2f_4 - f_1)U}{f_1 \lambda} \tag{5}$$

$$\frac{dU}{dx} + H\frac{dh}{dx} + G = 0 \tag{6}$$

The notation H and G are defined as follows:

$$H = \frac{f_1 U + \lambda A_2}{f_1 h + \lambda U(2f_4 - f_1)} \tag{7}$$

$$G = \frac{A_1 + \lambda A_3}{f_1 h + \lambda U(2f_4 - f_1)} \tag{8}$$

where $A_1 = -E_e U$; $A_2 = (f_4 - f_1 + f_5 R_i)\frac{U^2}{h}$; $A_3 = \frac{U^2}{h}\left\{R_i\left(\frac{f_5}{2}\frac{h}{B}\frac{dB}{dx} - f_2 \tan\theta\right) + f_b + E_e\right\}$;

$\lambda = \frac{h}{U}\frac{D_3 \pm \sqrt{D_1}}{D_2}$; $D_1 = f_4^2 - f_1^2 f_4 + f_1^2 f_5 R_i$; $D_2 = f_1 f_4 - 2f_4 + f_1 - f_1 f_5 R_i$; $D_3 = f_1 - f_4$.

These equations model the motion of the body part, at the same time yielding the boundary conditions for solving the front part at the downstream end of the body part.

Next, with reference to Fig.1, where the frame of reference is such that the centre of gravity of the front is stationary, a model to describe the motion of the front will be derived. Of particular importance in the modeling of the front flow are instantaneous volume balance due to the amount of entrainment q_e in the front part, the amount of influx q_i from the body part to the front part, and the amount of efflux q_o from the front part caused by the dense fluid mixed out of the front by the less dense fluid. The expressions regarding volume flux are as follows:

$$q_e = E_d U_f L \quad (9) \; ; \quad q_i = h(U - U_f) \quad (10) \; ; \quad q_o = (h_f - h)(U_f - U_m) \quad (11)$$

Corresponding buoyancy fluxes(q_{Be}, q_{Bi}, q_{Bo}) are given, respectively, by

$$q_{Be} = 0 \quad (12) \; ; \quad q_{Bi} = Bh(U - U_f) \quad (13) \; ; \quad q_{B0} = B_m(h_f - h)(U_f - U_m) \quad (14)$$

In the preceding equations the velocity and buoyancy force correction factors(k_U, k_B) for the mixed layer are introduced and are defined by

$$k_U = \frac{U_f - U_m}{U_f} \quad (15) \; ; \qquad k_B = \frac{B_m}{B_f} \quad (16)$$

In addition, relationships on the geometry of the front are required for the modeling. A number of experimental results in an equilibrium condition shows that for a given bottom slope the geometry of the front holds approximately a similarity shape in the downstream direction, provided localized instantaneous protrusions are averaged out. Both the length-to-height ratio f and the volume correction factor S are known experimentally to be functions

of θ only.

$$f(\theta) = \frac{h_f}{L} \qquad (17)\ ; \qquad S(\theta) = \frac{A}{h_f L} \qquad (18)$$

Under Boussinesq's approximation the momentum equation governing the motion of the front flow is given by

$$F_p + F_g + F_d + M_{in} = \frac{d}{dt}\{S(\theta)(1+A_m)\rho_a L h_f U_f\} \qquad (19)$$

where F_p=hydrostatic pressure component; F_g=body force component; F_d=total drag force component; M_{in}=net inflow momentum from the body part; A_m=added mass coefficient. Eq.19 becomes

$$\frac{d}{dt}\{(1+A_m)S(\theta)U_f h_f^2\} = \{g(S(\theta)-1) + S(\theta)B_f\}h_f^2 \sin\theta + f(\theta)\{\frac{1}{2}k_B B_f(h_f^2-h^2)\cos\theta + \frac{1}{2}Bh^2\cos\theta + \left(1+\frac{B}{g}\right)h(U-U_f)^2 - k_U^2\left(1+\frac{k_B B_f}{g}\right)(h_f-h)U_f^2 - C_d U_f^2 h_f\} \qquad (20)$$

where C_d=drag coefficient; $\Delta\rho_m=\rho_m-\rho_a$; $\Delta\rho=\rho-\rho_a$.
The conservation of volume and mass are given respectively by

$$\frac{d}{dt}(S(\theta)h_f^2) = f(\theta)\{(U-U_f)h - k_U U_f(h_f-h)\} + E_d U_f h_f \qquad (21)$$

$$\frac{d}{dt}(S(\theta)B_f h_f^2) = f(\theta)\{B(U-U_f)h - k_U k_B B_f U_f(h_f-h)\} \qquad (22)$$

The propagation speed U_{fe} at the foremost point of the front is due to both U_f and the rate of expansion of the front part. Therefore, an appropriate expression for U_{fe} is given as,

$$U_{fe} = U_f + \frac{1}{f(\theta)}\frac{dh_f}{dt} \qquad (23)$$

In line with our interest in the practical aspects of modeling, to predict evolution of velocity, height, and density in the flow direction is more significant than the actual shape of the front. In this study, it is assumed that the geometry of the front is of rectangular shape and thus S(θ) =1, which appears to be a viable alternative for a wide range of bottom slopes although the shape of the front can be descrived as a quarter-ellipse when θ is less than 10° and a half-ellipse when θ =10~90° (Akiyama *et al.*(4)). This implies that model constants to be calibrated, i.e., C_d and k_U include the effects resulting from simplification of the front shape.

The added mass M' for a rectangular solid body may be given by

$$M' = \frac{1}{4}\rho_a P\pi h_f^2 \qquad (24)$$

where the coefficient P depends on f(θ) and is approximately given by Eq. 25. An added mass coefficient A_m is then expressed by Eq.26.

$$P = 2.433 - 2.585f(\theta) + 2.205f^2(\theta) \qquad (25)\ ; \qquad A_m = \frac{1}{4}P\pi f(\theta) \qquad (26)$$

Eqs. 20~23 model the behavior of the front part of an inclined starting plume.

EMPIRICAL RELATIONSHIPS FOR MODEL FORMULATION

A series of experiments for a saline inclined starting plume was conducted using two experimental facilities; a small plexiglass wall flume(2.0m L, 0.36m D, 0.22m W) for steep slopes(θ =45° , 60° , 90°) and a large plexiglass wall flume(10.0m L, 1.0m D, 0.205m W) for mild slopes(θ =5° ,5.71° ,8.13° ,10° ,20°). In all cases, flow visualization technique using a VTR camera was employed to quantify such gross flow properties as the front propagation speed U_{fe}, the geometry of the front part, and the layer thickness h of the body part. Only in the case of θ =5.71° and 8.13° , such local flow properties as the vertical velocity profiles of the body part u as well as the front part u_f and the density profiles of the body part ρ as well as the front part ρ_f were measured at several different sections(see Akiyama *et al.*(4) for the detailed experimental conditions and method).

The model requires empirical relationships regarding the length-to-height ratio $f(\theta)$ as well as the entrainment functions(E_e,E_d). From the aforementioned experimental study, the following empirical functions were quantified on the basis of a large volume of experimental data;

$$f(\theta) = 0.0053\theta + 0.23 \qquad (27)$$

$$E_e = \frac{0.08 - 0.1R_i}{1 + 7R_i} \qquad (28)$$

$$E_d = 0.0045\,\theta \qquad (29)$$

where R_i is the overall Richardson number defined by

$$R_i = \frac{Bh\cos\theta}{U^2} \qquad (30)$$

Fig.2 shows the relatioship between $f(\theta)$ and θ. The dependence of $f(\theta)$ on θ is much stronger than that reported by Britter & Linden(5). Owing to difficulty in the determination of the length of the front part, existing data obtained for θ less than 5° show considerable scatter. Fig.3 shows the dependence of E_e on R_i-number. Therein, E_e-values estimated from the spatial growth rate dh/dx is denoted by the open square and E_e-values estimated from the method of moments using the velocity and density profiles by the open circle. The entrainment function proposed by Turner(10) is modified into the form of Eq.28, considering that both limiting cases at very large and small R_i-values yield the same values as the empirical equation proposed by Turner. It shows that Eq.28 reasonably agrees with the present experimental results. Fig.4 shows the dependence of E_d on θ. E_d increases about linearly with increasing θ.

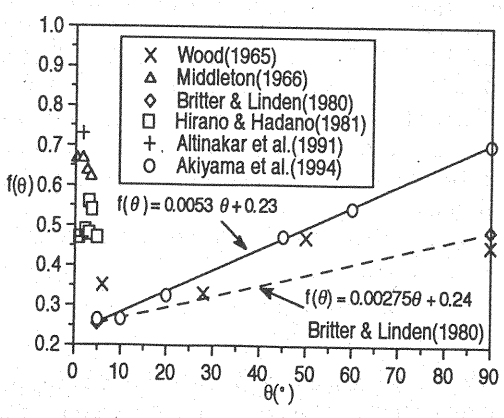

Fig.2 Dependence of $f(\theta)$ on θ.

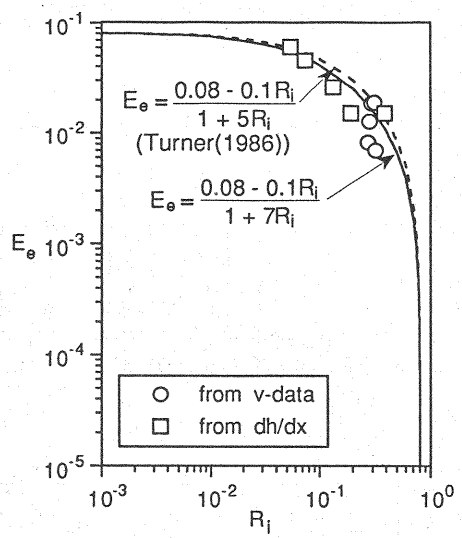

Fig.3 Entrainment Function E_e vs. R_i-number.

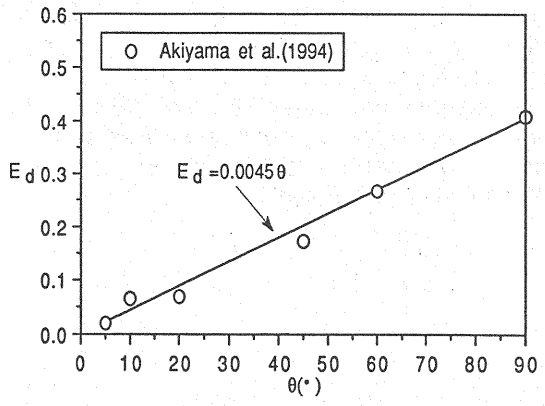

Fig.4 Entrainment Function E_d vs. θ.

MODEL CALIBRATION

The present model has been validated by calibrating it with experimental results. For the front part the drag coefficient C_d and the velocity correction factor k_U are treated as calibration coefficients, while for the body part the friction coefficient f_b is treated as a calibration coefficient. The buoyancy force correction factor k_B is set equal to zero, because the density of the mixed layer appears to be very small as indicated by very subtle difference in dh/dx-values between the body part of the inclined starting plumes and continuous inclined plumes(Ellison & Turner(6)). Consequently, in the present model the number of model constants are reduced to three for three conditions; the dimensionless front propagation speed U_{fe}^* (Fig.5) and the spatial growth rate dh_f/dx(Fig.6) are used to determine the values of C_d and k_U, while the spatial growth rate dh/dx(Fig.6) is used to determine the values of f_b. The motion of the body part of starting plumes travelling slope angles more than 5° appears to be free from that of the front part. Hence, the body part is first calibrated, and subsequently the front part is calibrated. The followings are the empirical results used for model calibration(Akiyama *et al.*(4));

$$U_{fe}^* = 1.34 \tag{31}$$

$$dh_f/dx = 0.0037\theta \tag{32}$$

$$dh/dx = 0.0009(\theta + 5) \tag{33}$$

The profile constants f_1, f_3, and f_4 set equal to 1.0. f_2=0.75 and f_5=0.25 are used in the model calibration as well as in all subsequent calculations. According to the study for continuous inclined plumes by Ellison & Turner(6), f_2 and f_5 typically vary from 0.6 to 0.9 and 0.2 to 0.3 respectivery for the range of bottom slope angles θ=5~90° . The values of f_2=0.75 and f_5=0.25 are selected based on the average of f_2- and f_5-values obtained by Ellison & Turner.

It is found from model calibration that in the range of bottom slope angles θ =5~90° , f_b = 0.01 and both k_U and C_d depend on θ as shown in Fig. 7. The comparison between the calculated and experimental results regarding U_{fe}^* , dh_f/dx, and dh/dx are also presented in Figs. 8 and 9, where the parameter k_U and C_d are selected to give satisfactory agreement with the experimental data. Therein, calculated values are denoted by open and closed circles and experimental results by solid lines presented in Figs. 5 and 6.

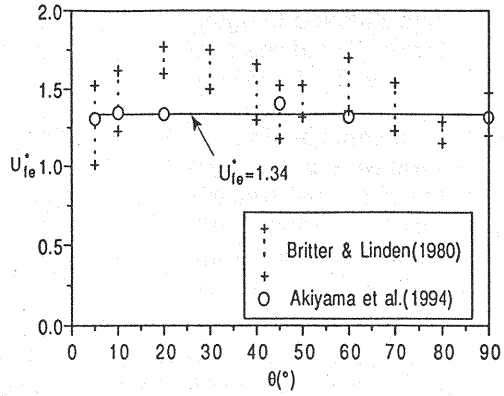

Fig.5 Comparison of U_{fe}^*-values.

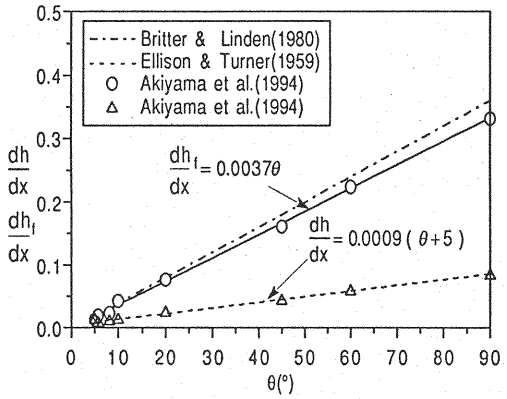

Fig.6 Comparison of dh/dx- and dh_f/dx-values.

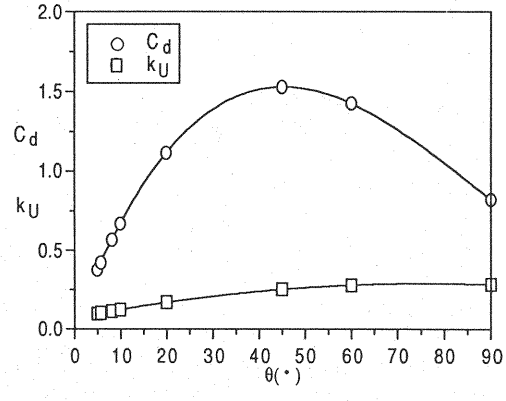

Fig.7 Calibrated C_d and k_U vs. θ.

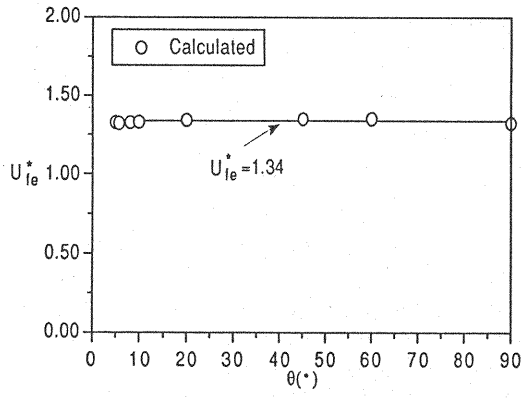

Fig.8 Comparison of Calculated U_{fe}^* with the Experimental Results.

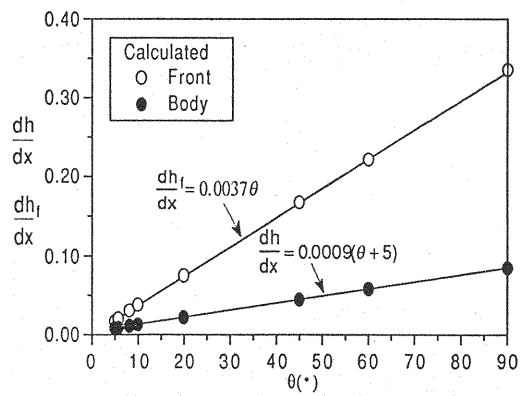

Fig.9 Comparison of Calculated dh_f/dx and dh/dx with the Experimental Results.

SAMPLE CALCULATION

The model is applied to hypothetical situations to examine quantitative performance of the model. The case in which a plume is set up by the release of constant buoyancy flux $q_{fi}(0,0)$ is examined, where $q_{fi}(x,t) = q(x,t)B(x,t)$. Keeping $q_{fi}(0,0)$ constant, three different inflow conditions given in Table 1 are considered. The case of the bottom slope angle $\theta = 5^\circ$ is simulated. Only the simulated results for condition 1 is presented in Fig.10 because the simuleted results for other conditions are qualitatively identical. As can be seen in this figure, U_{fe}~ constant, h_f~x, B_f~x, and R_{if} ~constant are predicted in the equilibrium stage, similar to continuous inclined starting plumes or the body part of inclined starting plumes. In continuous inclined plumes, a so-called normal condition exists, which is characterized by a constant overall Richardson number R_i at a given bottom slope angle. It is of particular significance to note that the overall Richardson number R_{if} of the front, defined by $B_f h_f \cos\theta / U_f^2$, becomes constant with respect to x. This implies that the front flow also attains an equilibrium condition.

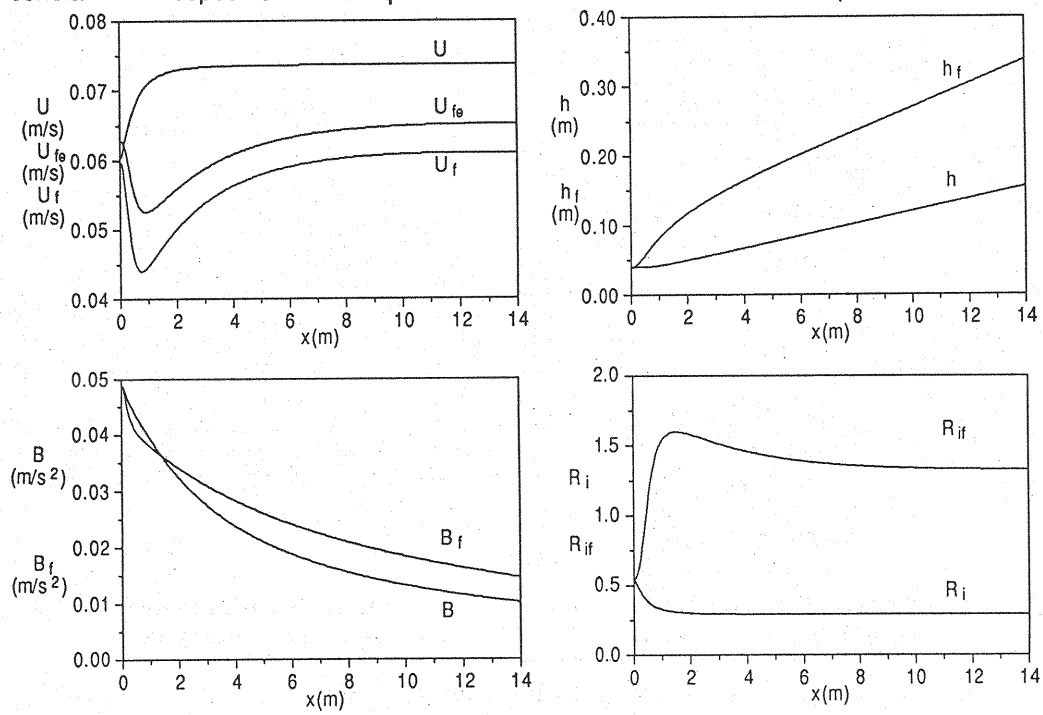

Fig.10 Simulated Results(Condition 1).

A significant but missing information in the existing literatures is the knowledge on buoyancy force B_f. Here, the dependence of the dimensionless spatial-decay-rate of buoyancy force B_f^*, defined by Eq.34, on θ is examined through numerical simulation.

$$B_f^* = \frac{h_f^2 dB_f/dx}{(q_0 B_0)^{2/3}} \qquad (34)$$

Table 1 Inflow Conditions for Simulation.

Upstream B.C.	U_0(m/s)	h_0(m)	ε_0
1	0.06	0.04	0.005
2	0.06	0.02	0.010
3	0.12	0.02	0.005

Fig.11 shows the variation of B_f^* in the flow direction. It shows that B_f^*-values, which is initially different(Table 1), converge into a unique value depending on a given θ. Fig.12 shows the relationship between B_f^* and θ, which decreases about linearly with θ.

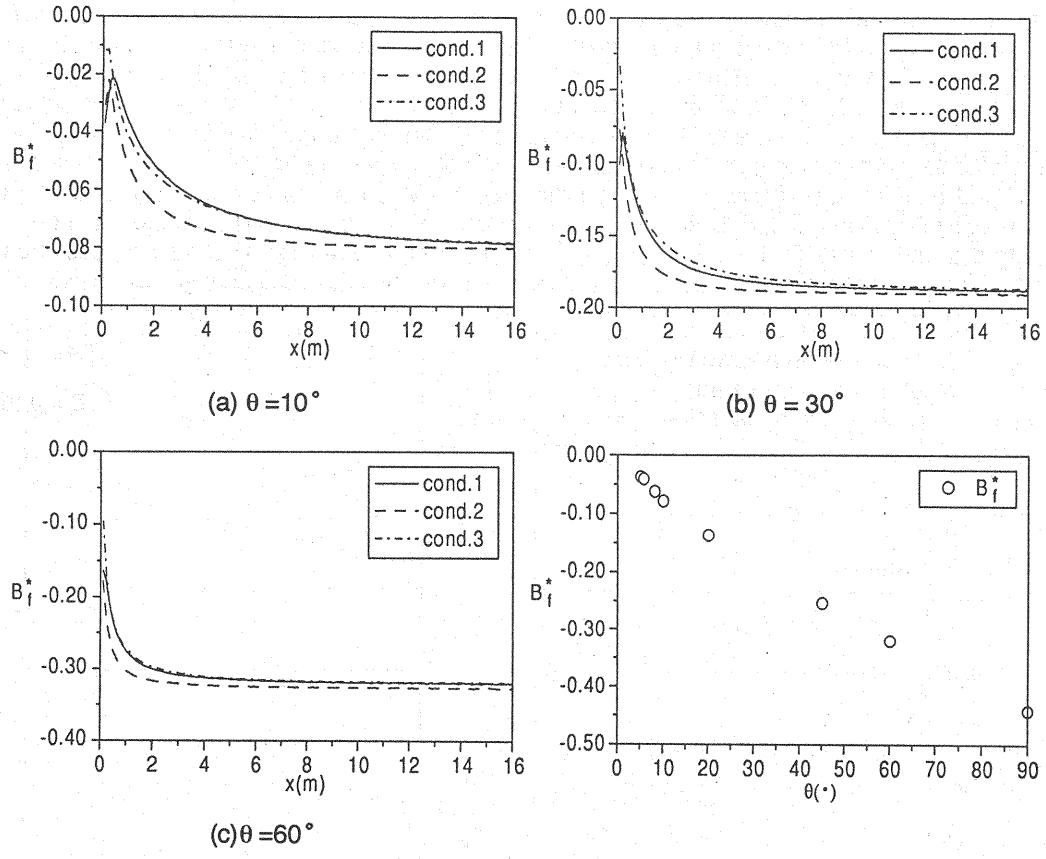

Fig.11 Dimensionless Spatial-Decay-Rate of Buoyancy Force B_f^* vs. x.

Fig.12 Dimensionless Spatial-Decay-Rate for Buoyancy Force B_f^* vs. θ.

COMPARISON WITH EXPERIMENTAL DATA

The inflow conditions such as q_0 and B_0 change due to dilution at the inlet. For computation, initial conditions are needed at a section x_i, where initial dilution is complete. Since the intial buoyancy flux $q_{fi}(0,0)$ is conserved independently of any mixing between the fluid occurring near the inlet for non-suspension inclined starting plumes, the conservation of volume and mass in the region of initial mixing yields $q_i=(1+\gamma)q_0$ and $B_i=B_0/(1+\gamma)$. The rate of initial dilution can be determined by estimating B_i experimentally. Once the flow thickness h_i at x_i is known, the average flow velocity U_i can be calculated by $U_i = (1+\gamma)\, q_0 / h_i$. Based on five measurements, the initial conditions(U_i, B_i, h_i) are obtained as follows; (U_i, B_i, h_i) = (6.84cm/s, 5.39cm/s^2, 5.0cm) for $\theta = 5.71°$ and (U_i, B_i, h_i)=(6.30cm/s, 7.35cm/s^2, 4.0cm) for $\theta = 8.13°$

In Fig. 13, the performance of the present model is tested against the experimental data. Variations of such flow characteristics as U_f, h_f, and B_f for the front part as well as U,h, and B for the body part in the flow direction are determined in case of $\theta = 5.71°$ and $8.13°$, using velocity and density distributions. The following model constants determined through model calibration are used in calculations; $C_d = 0.42$, $k_U = 0.10$, and $f_b = 0.01$ for $\theta = 5.71°$ and $C_d = 0.57$, $k_U = 0.12$, $f_b = 0.01$ for $\theta = 8.13°$. There exist, however, some noticiable differences between the calculated and experimental results. In particular, the predicted values of both B_f and B differ substantially from the experimental results. Such discrepancy is due partly to the modeling of the flow; the assumptious for the shape of the front part and profile constants for the body part are made. Another factor to cause discrepancy may be due to the error associated with experiments. In fact, it may be seen that the values of U_{fe}^* as well as dh_f/dx and dh/dx obtained for $\theta = 5.71°$ and $8.13°$ in an equilibrium stage are slightly different from those presented in Figs.5 and 6.

Measurements for velocity and density distributions of the front part at several different cross-sections are extremely difficult and time-consuming, due to unsteady nature of the flow. An effort was made to eliminate uncertainties associated with experiments by repeating the experiment under the same conditions. However, owing to the aforementioned exacting limitation in the experimental work, the data presented in Fig.13 were obtained by averaging only three experimental runs. In addition, as observed by a number of investigators, flow properties of the front oscillate as the flow travels downslope, due to intermittent loss of buoyancy to the wake of the front part. This gives rise to an additional uncertainty in the flow properties of the front part, which is, in fact, inherent in the phenomenon. Likewise, there exsits some uncertainty in the flow properties of the body part. This is caused by an uncertainty associated with entrainment and friction characteristics.

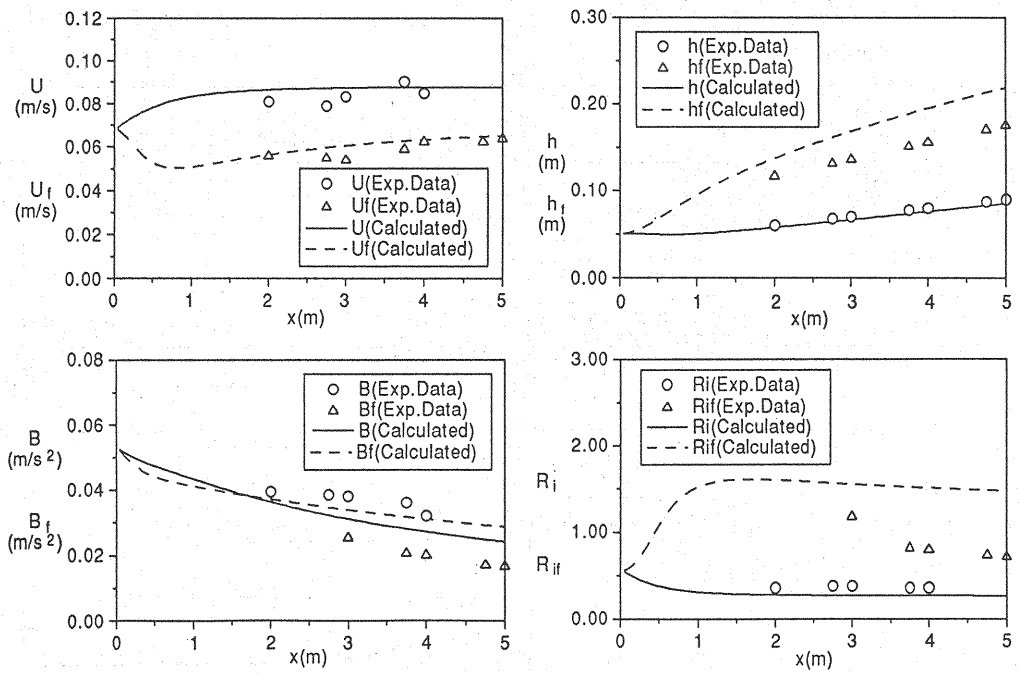

Fig.13 a Comparison of Calculated Results with Experimental Results Using Calibrated Model Constants($\theta = 5.71°$).

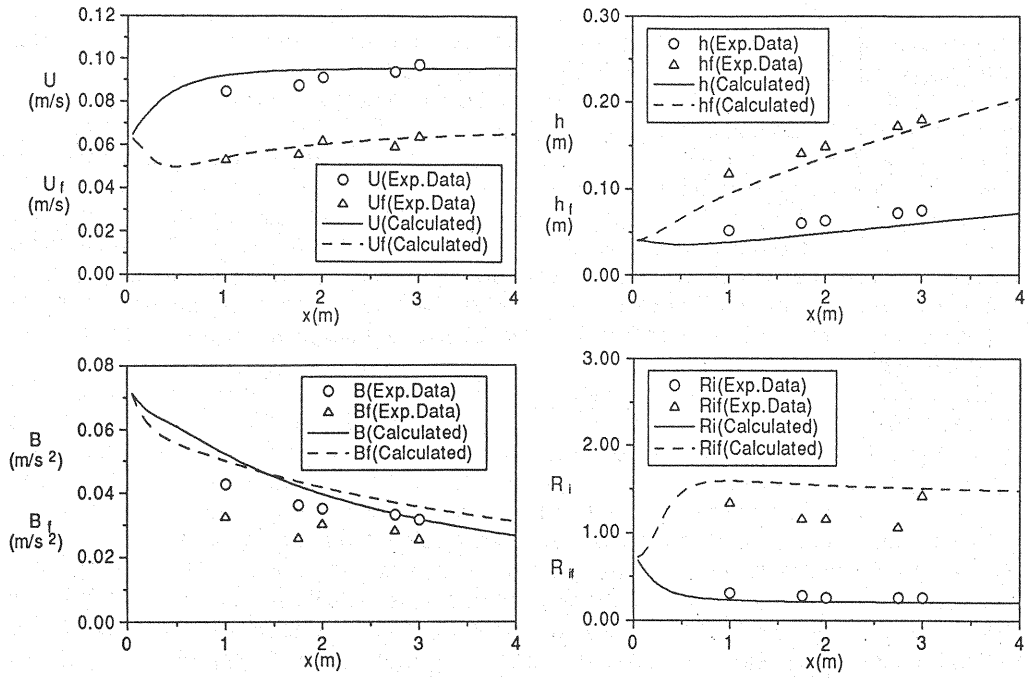

Fig.13 b Comparison of Calculated Results with Experimental Results Using Calibrated Model Constants(θ =8.13°).

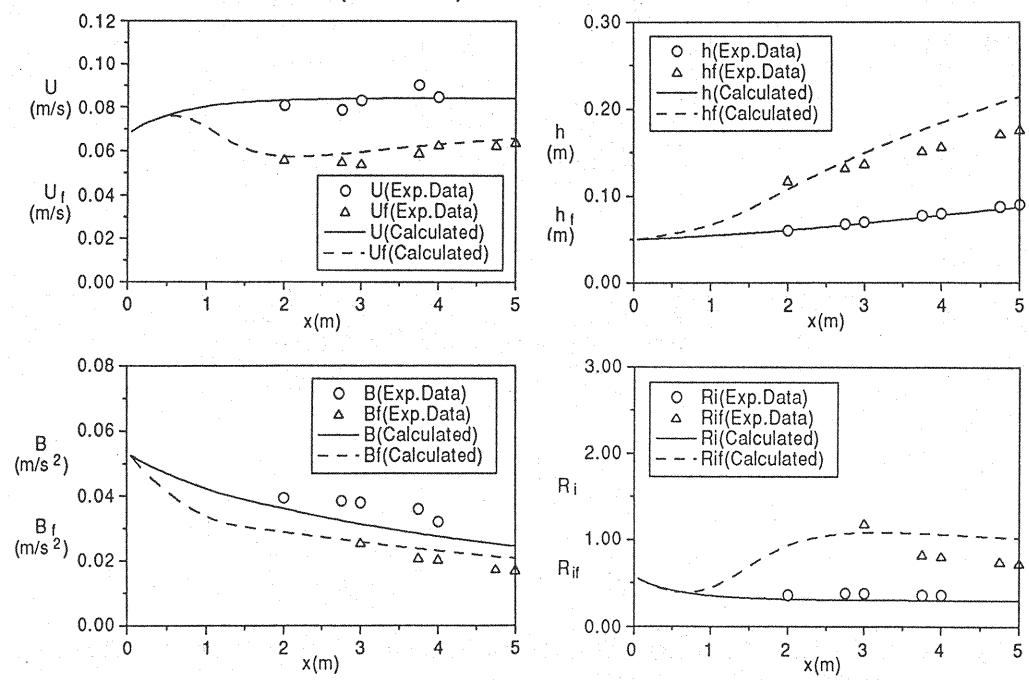

Fig.14 a Comparison of Calculated Results with Experimental Results Using Modified Model Constants(θ =5.71°).

CONCLUSIONS

A hybrid numerical model for an inclined starting plume is formulated on the basis of the characteristic method for the body part and the Runge-Kutta-Gill method for the front part, incorporating the empirical relationships for an entrainmnet function of the body part as well as the front part and the length-to-height ratio of the front part. To make the proposed model as universal as possible, for the range of bottom slope angles θ=5~90° the model constants are calibrated with the empirical relationships for the dimensionless front propagation speed and the spatial growth rate for the body part as well as the front part. The motion of the flow for θ=5.71° and 8.13° are examined in detail. Reasonable agreements between the calculated and experimental results are obtained, by modifying some of the calibrated model constants. To judge true applicability of the model for a wide range of bottom slope conditions such flow characteristics as velocity, density, and height of the front part are needed to be quantified experimentally with good accuracy.

ACKNOWLEDGEMENT

This study was partly supported by the Grant-in-Aid for Science Research(C) of the Ministry of Education and Culture, Japan under the Grant NO. 6650568.

REFERENCES

1. Akiyama,J., W. Wang and M. Ura: Numerical model of unsteady inclined plumes, Proceedings of Hydraulic Engineering, JSCE, Vol. 35, pp.167-172, 1991(in Japanese).
2. Akiyama,J. and M.Ura: Prediction of inclined starting plumes, Proceedings of Int'l Symposium on Environmental Hydraulics, Hong Kong, Vol.1, pp.59-64, 1991.
3. Akiyama,J.: Inclined starting plume and thermal(Sec.3.3), Journal of Hydroscience and Hydraulic Engineering, Research and Practice of Hydraulic Engineering in Japan, No.S1-1Hydraulics, pp.84-91,1993.
4. Akiyama,J., M.Ura and K.Sakamoto: Flow characteristics and entrainment of two-dimensional starting plumes travelling downslope, Journal of Hydroscience and Hydraulic Engineering, JSCE, 1994, in press.
5. Britter,R.E. and P.F. Linden: The motion of the front of a gravity current travelling an incline, Journal of Fluid Mechanics, Vol.99, pp.531-543,1980.
6. Ellison,T.H. and J.S. Turner: Turbulent entrainment in stratified flow, Journal of Fluid Mechanics,Vol.6,pp.423-448,1959.
7. Fukuoka,S., K. Mizumura and T. Kanoh: Fundamental study on dynamics the head of gravity current, Proceedings of JSCE, JSCE, Vol.274, pp.41-55, 1978(in Japanese).
8. Fukushima, Y: Analysis of two-dimensional density front with suspended solid materials, Proceedings of JSCE, JSCE, Vol.461, II-22, pp.21-30,1993(in Japanese).
9. Hirano,M and K. Hadano: Characteristics of motion of density current head, proceedings of JSCE, JSCE, Vol.314, pp.67-73, 1981(in Japanese).
10. Turner,J.S.: Turbulent entrainment: the development of the entrainment assumption, and its application to geophysical flows, Journal of Fluid Mechanics, Vol.173, pp. 431-471, 1986.

APPENDIX-NATATION

The following symbols are used in this paper:

A =volume of the front part per unit width;
B =layer averaged buoyancy force;
b =local buoyancy force;
E_e =entrainment function for the body part;
E_d =entrainmnet function for the front part;
$f_{i=1\sim5}$ =profile constants for the body part;
$f(\theta)$ =length-to-height ratio of the front;
g =acceleration due to gravity;
h =flow thickness;
k_U =velocity correction factor in the mixed layer;
k_B =buoyancy force correction factor in the mixed layer;
L =length of the front part;
M' =added mass;
P =coefficient related to added mass;
q_e =amount of entrained fluid in the front part;
q_i =amount of influx from the body to the front part;
q_o =amount of efflux from the front to the mixed layer;
q_{fl} =buoyancy flux;
R_i =overall Richardson number;
$S(\theta)$ =shape factor of the front part;
U =layer averaged flow velocity;
u =x-local velocity; and
v =y-local velocity.

Subscript

a =refers to ambient fluid;
f =refers to property of the front part;
f_e =refers to property of the foremost point of the front;
i =refers to property at the initial point;
m =refers to mixed layer; and
0 =refers to property at upstream boundary.

Superscript

$*$ =refers to dimensionless property.

Greek

δ =width of plume;
ε =relative density difference;
γ =rate of initial dilution;
θ =bottom slope in degree; and
ρ =density of fluid.